An analysis and verification of a dynamical model of a transverse flux motor

Marian Łukaniszyn, Marcin Kowol, Janusz Kołodziej
Opole University of Technology
45-272 Opole, ul. Sosnkowskiego 31, e-mail: m.lukaniszyn; m.kowol; ja.kolodziej@po.opole.pl

The paper presents dynamics simulation results for the three-module reluctance motor (Transverse Flux Motor -TFM) with an outer rotor. Calculations of the most important integral parameter used in the circuit model, are performed using the Flux3D package based on the finite element method. A mathematical model for a dynamics analysis of TFM is built in the Matlab/Simulink environment. The model has a hierarchical structure with its fundamental part being a single phase-belt of the motor. The basis for the construction of the laboratory setup is a DS1104 R&D Controller Board with a CP1104 Connector Panel. The experimental validation is divided into two parts. In the first step, the mathematical model of TFM under steady-state operation is examined. In the second step, experimental validation of the results obtained from the dynamical circuit models is performed. Results of the simulations, confirmed by the experimental validation presented in this work, allow to determine the most important characteristics of TFM in both dynamic and steady-state conditions.

1. Introduction

Transverse flux motors (TFMs) have recently attracted remarkable interest both from the academia and various industrial environments [1, 3, 5, 6, 9, 10, 11]. The low-speed motor is characterized by a high ratio of the electromagnetic torque to its volume [2, 4, 11], leading immediately to various high-torque transmission-free applications, to mention electric wind generators [1], electric (and hybrid) drives [11] and in-wheel drives [3, 9].

Our previous papers on TFM's have been devoted to the problem of reduction of accompanying torque pulsations, which have been plaguing not only TFM's [2, 4, 5, 7]. Effective construction optimization tools have been offered in order to reduce the torque pulsations while maintaining a high level of the average electromagnetic torque [5, 7].

In this paper, we extend our TFM modeling and simulation interest to include dynamical states of the motor, which is justified mainly by the start-up operating conditions, the switches in the supply bridge and possible changes in the load.

2. Prototype of TFM

The main object of the research is switched reluctance motor with axial flux (TFM). The prototype motor structure is shown schematically in Fig. 1. The

considered motor consists of three modules in which the rotors are shifted by 10 mechanical degrees with respect to each other. The stator modules are placed symmetrically on an acid-resistant steel shaft. Each module has twelve teeth and includes one phase belt that forms a solenoid. The rotor teeth are made of solid iron. The modules are insulated by nonmagnetic inserts. The outer layer and rotor layer are made of a nonmagnetic material (aluminium). The main specifications for the motor are given in Table 1.

Table 1. Specifications for TFM

Supply voltage	U_n=24V
Rated current	I_n=12A
Rotational speed	0÷300 obr/min
Winding	Three-phase
Number of turns	130
External diameter of rotor	158 mm
External diameter of stator	103.5 mm
Air gap	δ=0.5 mm

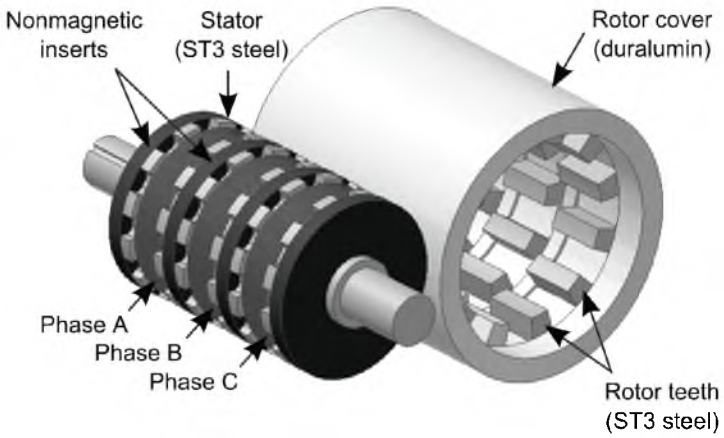

Fig. 1. TFM structure

A power converter (Fig. 2) is required to activate and commutate the SRM phases, and the classic asymmetric half-bridge inverter is in general used, requiring two switching devices and two power diodes per phase [4, 5]. There are two control procedures possible – *Hard-Chopping* and *Soft-Chopping*. The simplest motor control consists in sequentially switching *on* and *off* for the phase current (phases A, B, C, A etc.).

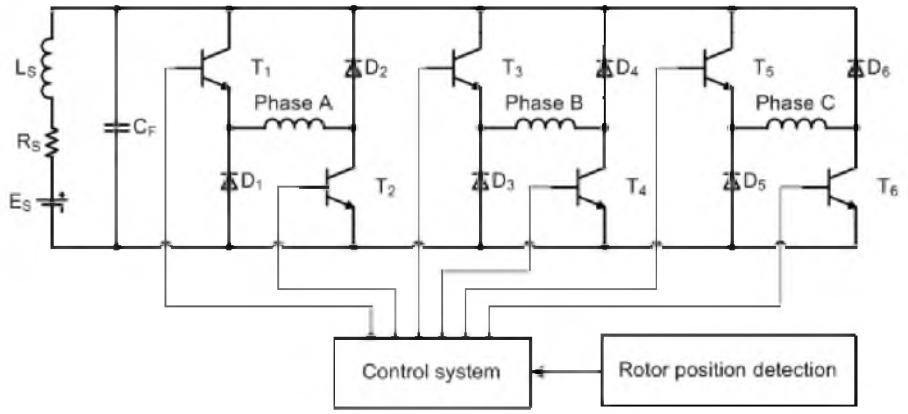

Fig. 2. The half-bridge ("H") TFM power converter

3. Circuit and field-circuit models

The modeling process for SRMs with axial flux is different from the techniques used in conventional cylindrical motors. The main reason for that is high nonlinearity of the reluctance motor. There are many interesting solutions for this type of problems in the bibliography [5, 10, 11, 12].

The dynamics of the motor can be described by two below equations presented. The first equation describes the electromagnetic phenomena

$$u_n(t) = R_n i_n(t) + \frac{d\psi_n(t)}{dt} \tag{1}$$

where $u_n(t)$ is the n-th phase supply voltage, R is the phase winding resistance, $i_n(t)$ is the n-th phase current and $\psi_n(t)$ is the flux in the n-th phase winding.

The second equation involves the nonlinear mechanical phenomena

$$T_e(t) = T_l(t) + k_\omega \omega(t) + J\frac{d\omega(t)}{dt}$$

$$T_e = \sum_{n=1}^{3} T_{en}(i_n, \Theta) \tag{2}$$

where $T_{en}(t)$ is the n-th phase electromagnetic torque, $T_l(t)$ is the load torque, $T_e(t)$ is the total electromagnetic torque, k_ω is the friction damping coefficient, J is the moment of inertia of the rotor , $\omega(t) = \frac{d\Theta(t)}{dt}$ is the angular rotor speed and $\Theta(t)$ is the rotor position.

Solution to these equations is easy under the linear model assumption for (2), at the cost, however, of considerable errors. The second way of solving these equations is to take into account the nonlinear flux and torque characters. The magnetostatic calculations are one of the methods for including the nonlinearity.

The nonlinear flux and torque characteristics $\psi = f_1(i,\Theta)$ and $T = f_2(i,\Theta)$, respectively, depending on current and rotor position, have been obtained from the MES field calculations verified by measurements on the prototype motor (see Fig. 3) [5].

The above mentioned software enables to solve the TFM transient-state problem after coupling an external power circuit with a control system. The nonlinear mathematical model (1) and (2) coupled with magnetostatic FEM is highly competitive with a possible use of the complicated, time-consuming FEM field-circuit model.

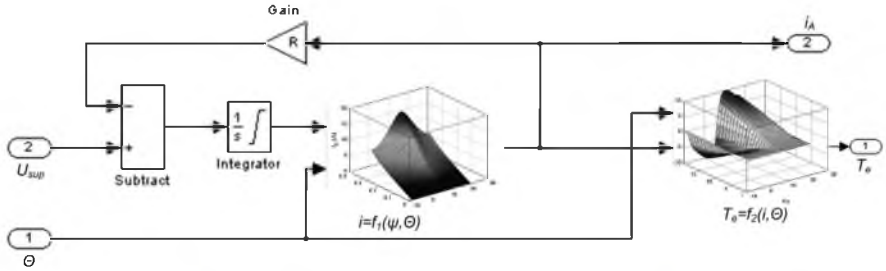

Fig. 3. Single phase subsystem

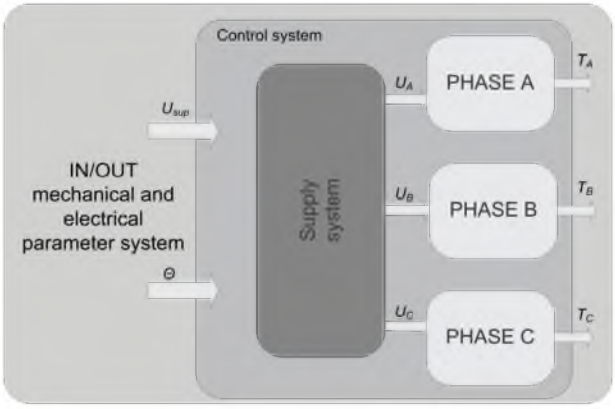

Fig. 4. The structure of a simulation system in Matlab/Simulink

The structure of a simulation system in Matlab/Simulink, presented in Fig. 4, is hierarchical. It consists of several units, the most important of which is a model of a single phase. All the belts are supplied from a power electronic supply system implemented in the Plecs environment (classical "H" half-bridge). The main supervisory system enables to introduce mechanical and electrical parameters related to the nature of simulations run, as well as output data acquisition.

4. Test bench

A laboratory stand for the TFM simulation test bench includes the DS1104 fast-prototyping card of dSPACE, cooperating with the PCI bus, the CP1104 input/output panel and auxiliary units like RTI and ControlDesk modules. The first module enables to create applications in Simulink from the graphics level while the second one provides on-line visualization of variables of interest. An easy access to the tools enabling to modify selected parameters during the simulation run is of importance as it is not necessary to change and re-generate a source code for the DSP processor.

A view of the laboratory stand and a block diagram of the simulation test bench for the TFM motor under test are shown in Figs. 5 and 6, respectively.

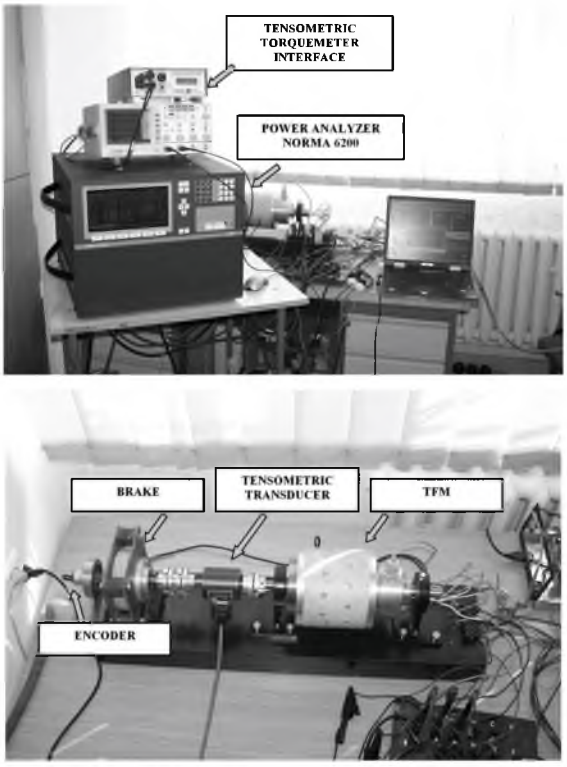

Fig. 5. The laboratory set of TFM

The test TFM is supplied from batteries. The torque is measured with the E300-RWT1-02 tensometric torque sensor. On-line measurements of angular position of the rotor with respect to the stator are performed by means of a rotational-pulse transducer with the resolution of 1000 pulse/rev. The TFM is loaded with an

electric dynamometer. For supervisory control, the above mentioned DS1104 card is applied, together with the CP1104 panel. The card also enables to measure both analog and digital signals. However, due to the lack of a separation system, measurements of currents and voltages in particular belts of the motor are performed by means of a 12-channel power analyzer.

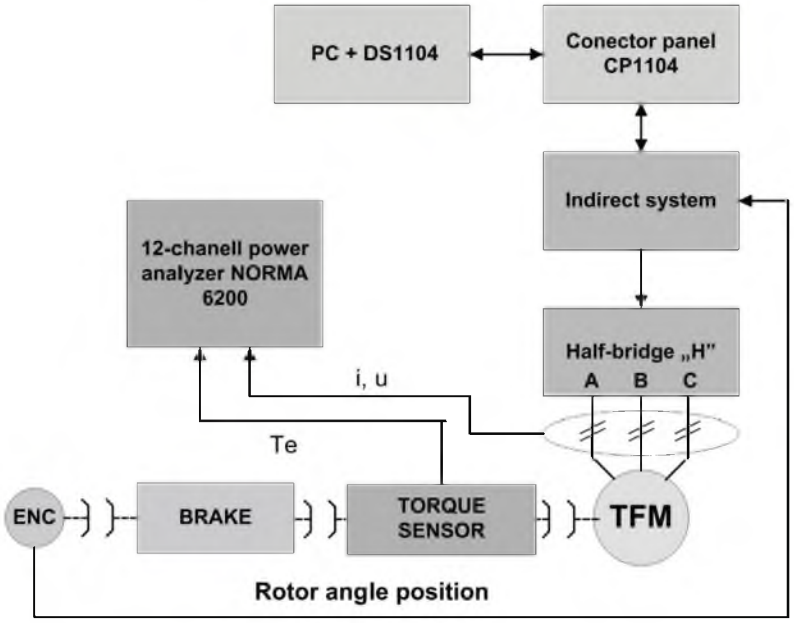

Fig. 6. The Block diagram of TFM test bench

5. Calculations and experimental validation

A due "closeness" of mechanical characteristics for the test TFM and its simulation model is selected as a criterion for the correctness of the model. A comparison of mechanical characteristics $n=f(T_l)$, where n is the rotational speed, for various switch-on (α_{on}) and switch-off (α_{off}) angles shows a good accuracy of the considered circuit model (Fig. 7).

In the next part of this work, TFM simulation and experimental verification results will be presented in case of the motor start-up under load. To this end, Fig. 8 presents plots of currents and voltages drop in each particular phase belt in case of 1) measured ones in the test TFM (with the NORMA 6200 power analyzer), 2) obtained from the circuit model (Matlab/Simulink) and 3) obtained from the field-circuit model (Flux3d). Comparison of source current and electromagnetic torque for the measurements, circuit and field-circuit models at the supply voltage U_{sup}=12V, load torque T_l=0,7 N·m, α_{on}=18°, α_{off}=28°are shown additionally in Fig. 9.

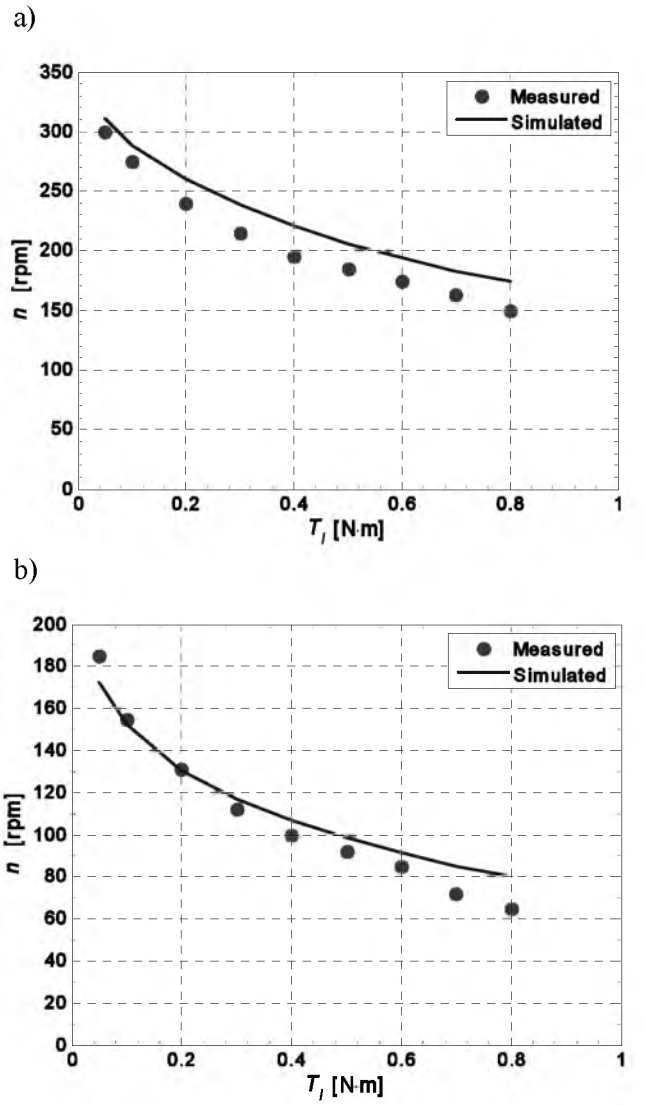

Fig. 7. Mechanical characteristics: a) α_{on}=17°, α_{off}=27°, U_{sup}=24V b) α_{on}=17°, α_{off}=27°, U_{sup}=12V

Quite slight discrepancies of some 5% to 15% between the measurements and simulations for the finally accepted circuit model result mainly from the simplifying assumptions made. In fact, magnetic couplings between the adjacent modules have been omitted in the model. Also, the influence of temperature changes on resistance of windings for each particular phase belt as well as possible induction of eddy currents in solid parts of the rotor and stator have not been accounted for.

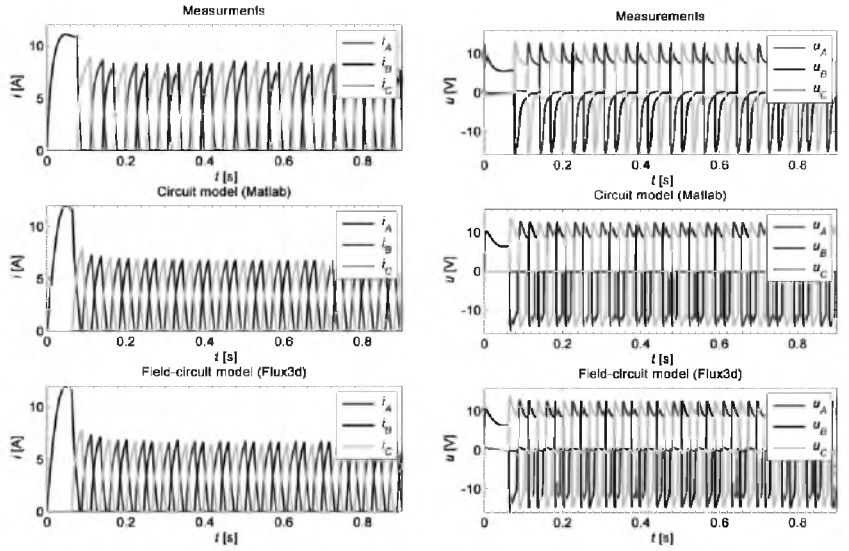

a) b)

Fig. 8. Comparison of phase currents a) and voltage drop b) for measurements, circuit and field-circuit models, at the supply voltage U_{sup}=12V, load torque T_l=0,7 N·m, α_{on}=18°, α_{off}=28°

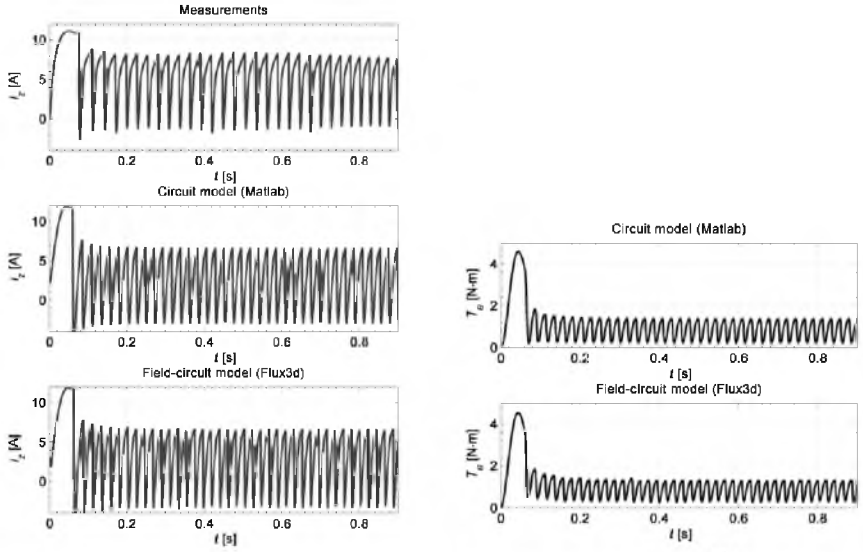

a) b)

Fig. 9. Comparison of source current a) and electromagnetic torque b) for the measurements, circuit and field-circuit models at the supply voltage U_{sup}=12V, load torque T_l=0,7 N·m, α_{on}=18°, α_{off}=28°

Fig. 10 presents plots of phase belt currents under step change in load. After a no-load start-up, at time t_1=2s the motor is step-wise loaded with the moment T_l=1 N·m. At time t_2=3s, the load is coming back to T_l=0 N·m. Rotational speed at the step change of load torque for various supply voltages and α_{on}=17°, α_{off}=27° are shown additionally in Fig. 11.

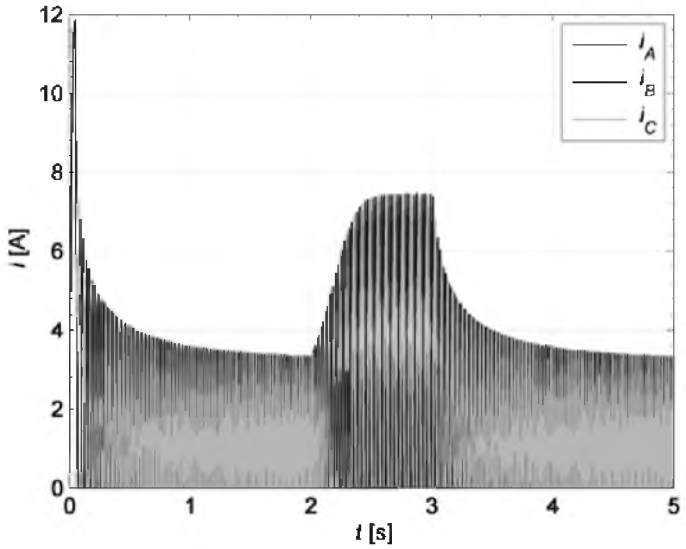

Fig. 10. Currents of phases A, B, C for a step change of load torque at supply voltage U_{sup}= 12V and α_{on}=17°, α_{off}=27°

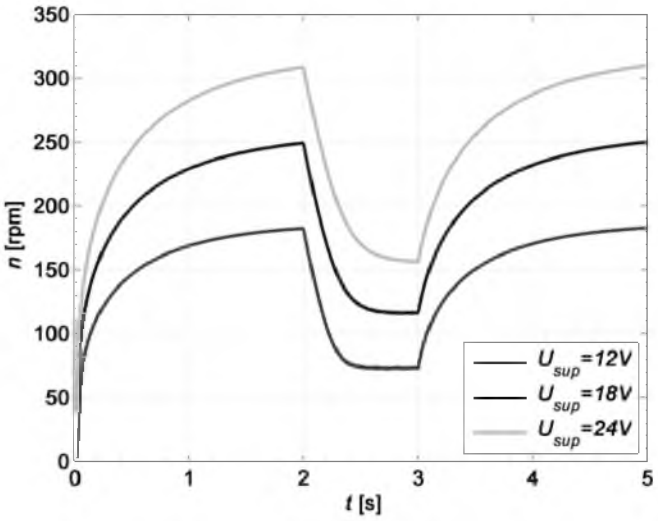

Fig. 11. Rotational speed at the step change of load torque for various supply voltages and α_{on}=17°, α_{off}=27°

6. Conclusions

The developed nonlinear, dynamic circuit model of transverse flux motor has been shown in simulations and experimental verification to have a good accuracy. The model enables a fast analysis of the motor operation and it is competitive with respect to a field-circuit model. In addition to the construction optimization methodology for the TFM offered earlier [6, 7], the nonlinear dynamic model presented here, supports analysis and design tools for the TFM.

Further research works in the field will be focused on an analysis of influence of control algorithms on the electromechanical parameters of TFM as well as control optimization in order to reduce torque pulsations and to increase the efficiency of TFM.

References

[1] Arshad W. M., Thelin P., Bäckström T., Sadarangani C.: Use of Transverse-Flux Machines in a Free-Piston Generator, IEEE Transactions on Industry Applications, July/August 2004, vol. 40, No. 4, pp. 1092÷1100.

[2] Babazadeh A., Parspour N., and Hanifi A.: Transverse flux machine for direct drive robots: Modelling and analysis, IEEE Conference on Robotics, Automation and Mechatronics, Singapore, vol. 1, 2004, pp. 376- 380.

[3] Goryca Z., Łukaniszyn M., Jagiela M., Wróbel R.: Analiza momentu elektromagnetycznego w silniku reluktancyjnym, XXXIX SME, Cedzyna/Kielce 2002, pp. 333÷339.

[4] Kastinger G.: Design of a novel transverse flux machine, ICEM 2002, Brugge, August 2002.

[5] Kołodziej J.: Analiza dynamicznych i ustalonych stanów pracy silnika reluktancyjnego ze strumieniem poprzecznym, Praca Doktorska, Opole, 2011.

[6] Kowol M., Łukaniszyn M., Latawiec K.: Modeling and construction optimization of a modular TFM with an outer rotor. Electrical Engg., Vol. 92, No 3, September 2010, pp.111-118.

[7] Kowol M.: Analiza pracy przełączalnego silnika reluktancyjnego z wirnikiem zewnętrznym do napędu lekkich pojazdów, Rozprawa doktorska, Opole, 2007.

[8] Łukaniszyn M., Kowol M.: Analiza pracy modułowego silnika reluktancyjnego z wirnikiem zewnętrznym, Śląskie Wiadomości Elektryczne, 4'2005, s. 4-7.

[9] Łukaniszyn M., Kowol M.: Wpływ zmian konstrukcyjnych na parametry elektromechaniczne silnika reluktancyjnego z wirnikiem zewnętrznym, Przegląd Elektrotechniczny, Vol. LXXXII, No. 11, Sigma-NOT, 2006, pp. 43-45.

[10] Peethamparam A.: Design of Transverse Flux Machines using Analytical Calculations & Finite Element Analysis, March 2001 PhD Thesis, Royal Institute of Technology, Stockholm.

[11] Ritchie E., Tutelea L.: An overview of electric vehicle in-wheel drive systems, XXXIX Międzynarodowe Sympozjum Maszyn Elektrycznych, 9-11 June 2003, Gdańsk-Jurata, pp. 1-21.

[12] Tomczewski K., Wróbel K.: Jednoczesna optymalizacja kształtu obwodu magnetycznego i parametrów zasilania przełączalnego silnika reluktancyjnego, Przegląd Elektrotechniczny, 03/2009, s. 107-110.